^{1}H and ^{31}P NMR of Pentaammineruthenium(III) Complexes of Exocyclically-Coordinated Adenine and Cytosine Ligands. Evidence for Rotamers with Distinct Acidities

V. M. Rodriguez-Bailey and M. J. Clarke*

Merkert Chemistry Center, Boston College, Chestnut Hill, Massachusetts 02167

Received August 20, 1996[⊗]

^{1}H NMR spectra of the paramagnetic complexes [L$(NH_3)_5Ru^{III}$], where L = derivatives of cytosine-κ^{N4} and adenine-κ^{N6}, reveal rotameric isomers with distinct acid−base equilibria. ^{31}P NMR spectra of the 5′CMPκ^{N4} and 5′AMPκ^{N6} complexes indicate little interaction between the metal and phosphate centers. Differences between the ^{1}H and ^{31}P NMR of endo- and exocyclically-coordinated nucleosides and nucleotides are discussed and provide a means of distinguishing exocyclic from endocyclic nitrogen coordination.

Introduction

The growing interest in the interactions between ruthenium complexes and nucleic acids and their constituent bases derives from both the pharmaceutical properties of this metal[1−4] and its ability to function as an active center in chemical nucleases.[5] Delineating the NMR of paramagnetic Ru^{III} complexes with nucleic acid components provides a basis for using this spectroscopy to probe the mechanism of action of such anticancer compounds as *cis*-[$Cl_2(NH_3)_4Ru^{III}$][4,6] and *trans*-[(imidazole)$_2Cl_4Ru^{III}$].[2] Monodentate complexes of [$(NH_3)_5$-Ru^{III}] provide a relatively simple system for study, with a sufficient number of well-characterized examples to provide reliable structural data.[7,8] Complexes of this type with adenine and cytosine ligands (see Figure 1) are unusual in that Ru^{III} displaces a proton from the exocyclic amine (N_{exo}) of these bases (N6 of adenine and N4 of cytosine) to form amido complexes at neutral pH (see Figures 2 and 3).[7] Adding this proton back to the coordinated ligand occurs at the adjacent pyrimidine ring nitrogen (N_{endo}; N1 of adenine and N3 of cytosine), which then interferes with hydrogen-bonding interactions between the coordinated ammines and N_{endo}. Such interactions affect the rotameric configuration of the metal center around the C−N_{exo} bond. The ^{1}H NMR of these complexes as a function of pH allows the acid−base properties of the rotamers to be individually assessed, while the ^{31}P NMR can reveal interactions between the metal ion and the phosphate.

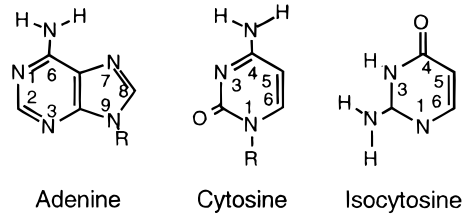

Figure 1. Structures and numbering system for adenine, cytosine, and isocytosine.

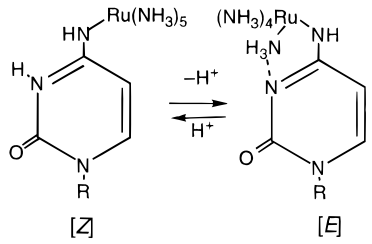

Figure 2. Rotameric structures in [(Cytκ^{N4})$(NH_3)_5Ru^{III}$].

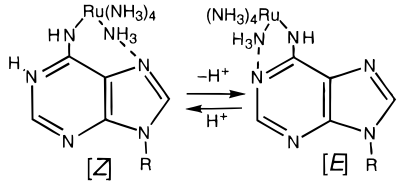

Figure 3. Rotameric structures in [(Adoκ^{N6})$(NH_3)_5Ru^{III}$].

Experimental Section

Materials and Synthesis. Ligands (Ado, adenosine; 1MeAdo, 1-methyladenosine; 8-D-Ado, 8-deuterioadenosine; 5′dAdo, 5′-deoxyadenosine; Ade, adenine (6-aminopurine); 5′AMP, 5′-adenosine monophosphate; Tub, tubercidin (7-deazadenosine); Cyd, cytidine; 1MeCyt, 1-methylcytosine; 1,5Me_2Cyt, 1,5-dimethylcytosine; 6MeICyt, 6-methylisocytosine = 2-amino-4-hydroxypyrimidine) were obtained from Aldrich or Sigma and used without further purification. Pentaammineruthenium(III) complexes of these ligands were prepared by previously reported methods involving direct combination with [$(H_2O)(NH_3)_5Ru]^{2+}$ followed by air oxidation and chromatographic purification.[7] Purities of all complexes were verified by HPLC on a C_{18} column with 10% methanol in 0.5 M ammonium propionate as the eluent. The free ligand often appeared as a contaminant and polynuclear complexes occasionally formed on standing. These were removed by further chromatographic purification on a Dowex-50 or Biorex-70 column eluted with HCl or ammonium formate, respectively. For nucleotidyl complexes, purity was most conveniently determined by ^{1}H and ^{31}P NMR. 8-D-Ado was prepared by boiling 250 mg of adenosine in 5.0 mL of 99.8% D_2O at 105 °C for 5 h, after which it crystallized on cooling.[9] [(8-D-Adoκ^{N6})$(NH_3)_5Ru]Cl_2$ was prepared and purified analogously to the undeuterated complex;[7] however, the

[⊗] Abstract published in *Advance ACS Abstracts,* March 15, 1997.

(1) Farrell, N. *Transition Metal Complexes as Drugs and Chemotherapeutic Agents*; Kluwer Academic: Boston, 1989.
(2) Keppler, B. K. *Metal Complexes in Cancer Chemotherapy*; VCH: Weinheim, Germany, 1993; p 429.
(3) Clarke, M. J. *Prog. Clin. Biochem. Med.* **1989**, *10*, 25−39.
(4) Clarke, M. J.; Stubbs, M. *Met. Ions Biol. Syst.* **1996**, *32*, 727−780.
(5) Pyle, A. M.; Barton, J. K. In *Bioinorganic Chemistry*; Lippard, S. J., Ed.; Wiley: New York, 1990; Vol. 38, pp 413−474.
(6) Clarke, M. J. *Ruthenium and Other Non-Platinum Metal Complexes in Cancer Chemotherapy*; Springer-Verlag: Heidelberg, Germany, 1989; Vol. 10.
(7) Clarke, M. J. *J. Am. Chem. Soc.* **1978**, *100*, 5068−5075.
(8) Graves, D. J.; Hodgson, D. K. *J. Am. Chem. Soc.* **1979**, *101*, 5608−5612.
(9) Schweizer, M. P.; Chan, S. I.; Helmkamp, G. K.; T'so, P. O. P. *J. Am. Chem. Soc.* **1964**, *86*, 696−700.

S0020-1669(96)01014-2 CCC: $14.00

solid product was redissolved in D_2O and rotary-evaporated to dryness again to minimize the proton content of the sample.

NMR. For routine spectra, 10 mg samples were lyophilized three times in 99.8% D_2O (Aldrich) to minimize the proton concentration and then dissolved in 0.6 mL of 100% D_2O ([Ru] $\approx$ 40−50 mM). Spectra were recorded on a Varian XL-300 NMR spectrometer using 5 mm oven-dried NMR tubes at 18.8 °C. A 100 ppm (+50 to −50 ppm) spectral width and a 5.00 Hz bandwidth were normally employed in obtaining one-dimensional ^{1}H spectra. The intense HOD solvent resonance was suppressed by the WEFT technique.[10,11] Proton chemical shifts were measured relative to TSP. The effects of intermolecular paramagnetic interactions were assessed by recording the spectra of representative complexes as a function of concentration from 20 to 220 mM. Concentration effects were usually less than ~0.2 ppm and were always considerably smaller than the intramolecular effects of the paramagnetic ion. NMR paramagnetic isotropic shifts were calculated as the difference between the observed shifts for a given proton in the complex and in the free ligand ($\delta_{iso} = \delta_{obs} - \delta_{dia}$, where δ_{dia} is that of the free ligand).

^{31}P NMR were recorded using the same probe and samples similarly constituted, but ~200 transients/sample were normally collected. ^{1}H NMR were recorded immediately prior to the ^{31}P spectra to ensure sample purity. The sweep width used was 60 ppm with phosphoric acid as an external standard.

T_1 measurements were generally made using the inversion recovery method; however, when paramagnetic line widths were large, the relationship $T_1 = T_2 = 1/\pi(\Delta\nu_{1/2})$ was used to estimate the relaxation time.[12] In order to eliminate the paramagnetic effects of dissolved oxygen, samples were purged with argon or subjected to freeze−thaw cycles under vacuum.

pH was adjusted with small amounts of DCl and NaOD (Aldrich) and the pH* (uncorrected pH) measured before and after each run with a combination glass microelectrode (Ingold Inc.). After standardization in pH 4 and 7 buffers, the pH electrode was soaked in D_2O prior to use. pK_a* values were derived from a least-squares fit of chemical shift versus pH* but are reported as pK_a values after conversion by the relations: p$K_a(D_2O)$ = pK_a* + 0.4 and p$K_a(H_2O)$ = (p$K_a(D_2O)$ − 0.45)/1.015 or pK_a = (pK_a* − 0.05)/1.015.[13] In cases where both rotamers were evident, an array of 10 spectra were obtained with a preacquisition delay of 10 s every 2 min until equilibrium was established.

Variations in the chemical shift for a given proton, when a single ionization was involved, were fit to the equation

$$\delta = \delta_a + \frac{(\delta_a - \delta_b)K_a}{[H^+] + K_a}$$

where δ_a is the chemical shift of the protonated form and δ_b is that for the ionized form. Titrations exhibiting two-proton equilibria were fit to the equation

$$\delta = \delta_1 + \frac{(\delta_2 - \delta_1)[H^+]K_{a1} + (\delta_3 - \delta_1)(K_{a1}K_{a2})}{[H^+]^2 + [H^+]K_{a1} + K_{a1}K_{a2}}$$

where δ_1, δ_2, and δ_3 are the NMR shifts corresponding to the forms H_2B, HB^-, and B^{2-}, respectively. K_{a1} and K_{a2} refer to the ionization of the first and second protons, respectively.

EPR measurements were made on a Varian E-9 spectrometer with ~4 mM complex in 50% ethylene glycol at −140 °C in 0.5 mm EPR quartz tubes.

Calculations of Paramagnetic Effects. Structural models were drawn using the PCMODEL and Chemdraw3D programs.[14,15] Owing to CPU constraints, the energies of $[(NH_3)_6Ru]^{3+}$, the individual heterocycles, and the sugar were individually minimized before construction and final minimization of the complexes. The most common conformations about the glycosyl bond (*syn* or *anti*), the sugar pucker (*C2′-endo*(*S*) or *C3′-endo*(*N*)), and the orientation about the C4′−C5′ bond (*gg*, *gt*, or *tg*)[16−22] were considered as possible structures. Structures were also generated from the X-ray crystal data of 5′AMP,[23] in which the sugar is *C3′-endo*,*anti*,*gg* and [(5′CMP)$(H_2O)Co^{II}$] is *C2′-endo*/*C1′-exo*,*anti*,*gg*.[24] Energy minimizations involving both adenosine[25] and cytidine[26] used the *C3′-endo*(*N*),*anti*,*gg* conformation, since the *syn* conformation of these nucleosides is rare. Since only approximations were sought, no attempt was made to average overall conformations of the sugar. It was also assumed that the heterocycle was positioned between the cis-ammine ligands, as is evident in the crystal structure of [(1MeCytκ^{N4})$(NH_3)_5Ru^{III}$].[8]

According to the treatment used for a similar series of ammineruthenium(III) complexes with heterocyclic ligands, dipolar contributions (δ_{dip}) were estimated from the following equation for $S = {}^1/_2$ at 292 K:[27]

$$\delta_{dip} = \frac{177.79}{r^3}(3\cos^2\theta - 1)(g_\perp{}^2 - g_\parallel{}^2) \qquad (1)$$

where r (Å) is the Ru−H distance and θ is the angle formed by the Ru−H vector and the Ru−N_{exo} axis.[27] Contact shifts were then estimated as $\delta_{con} = \delta_{iso} - \delta_{dip}$.

Calculated hyperfine coupling constants A_H for the base ring protons and A_N for the base ring atoms were obtained from ZINDO (INDO/1, UHF, doublet) calculations[28,29] on a CAChe workstation.[30] Where possible, calculations were done using crystallographic distances and angles; otherwise the structural parameters derived from geometries optimized by MM2[31] or INDO/1[28,29] energy minimization methods were used.

Results

NMR. Table 1 summarizes the ^{1}H NMR resonances for complexes of adenine and cytosine derivatives in which the metal ion is coordinated to the exocyclic nitrogen.[8] COSY spectra of the Adoκ^{N6} and dAdoκ^{N6} complexes are shown in Figures S1 and S2. ^{1}H NMR spectra of the Adoκ^{N6} and Cytκ^{N4} complexes as a function of pH are shown in Figures S3 and S4, while a plot of δ(H8) versus pH for the 5′AMPκ^{N6} complex is shown in Figure S5. Table S1 summarizes the calculated (INDO/1) A_H values for the ring protons in these complexes, and Figure S6 shows the distribution in signs for these hyperfine coupling constants around the heterocyclic rings of Cytκ^{N4} and Adoκ^{N6}. (Figures S1−S6 and Table S1 are given in the Supporting Information.)

(10) Patt, S. L.; Sykes, B. D. *J. Chem. Phys.* **1975**, *56*, 3182.
(11) Redfield, A. G.; Kunz, S. D.; Ralph, E. K. *J. Magn. Reson.* **1975**, *19*, 114.
(12) Drago, R. S. *Physical Methods in Chemistry*; W. B. Saunders: Philadelphia, PA, 1977.
(13) Martin, R. B. *Science* **1963**, *139*, 1198.
(14) Gilbert, K. E. *PCMODEL 1.0*, Serena Software: Bloomington, IN, 1988.
(15) Rubenstein, M.; Rubenstein, S. *Chemdraw3D*, 2nd ed.; Cambridge Scientific Computing, Inc.: Cambridge, MA, 1989.
(16) Orozco, M.; Velasco, D.; Canela, E. I.; Franco, R. *J. Am. Chem. Soc.* **1990**, *112*, 8221−8229.
(17) Altona, C.; Sundaralingam, M. *J. Am. Chem. Soc.* **1972**, *94*, 8205−8212.
(18) Saenger, W. *Principles of Nucleic Acid Structure*; Springer-Verlag: New York, 1984; p 556.
(19) Stolarski, R.; Pohorille, A.; Dudycz, L.; Shugar, D. *Biochim. Biophys. Acta* **1980**, *610*, 1−9.
(20) Davies, D. *Prog. NMR Spectrosc.* **1978**, *12*, 135−225.
(21) Guschlbauer, W. *Biochim. Biophys. Acta* **1980**, *610*, 47−55.
(22) Gelbin, A.; Schneider, B.; Clowney, L.; Hsieh, S.-H.; Olson, W. K.; Berman, H. M. *J. Am. Chem. Soc.* **1996**, *118*, 519−529.
(23) Kraut, J.; Jensen, L. H. *Acta Crystallogr.* **1963**, *16*, 79.
(24) Clark, G. R.; Orbell, J. D. *Acta Crystallogr.* **1978**, *B34*, 1815−1822.
(25) Lai, T. F.; Marsh, R. E. *Acta Crystallogr.* **1972**, *B28*, 1982−1989.
(26) Furberg, S.; Petersen, C. S.; Rømming, C. *Acta Crystallogr.* **1965**, *18*, 313−320.
(27) Bertini, I.; Luchinat, C. *NMR of Paramagnetic Molecules in Biological Systems*; Benjamin Cummings: San Francisco, CA, 1986; p 36−38.
(28) Bacon, A. D.; Zerner, M. C. *Theor. Chim. Acta* **1979**, *53*, 21−54.
(29) Sadlej, J. *Semi-Empirical Methods of Quantum Chemistry*; PWN-Polish Scientific Publishers and John Wiley and Sons: Warsaw, New York, 1985; pp 208−294.
(30) CAChe Scientific. *CAChe*; TekGraphics: Beverton, OR, 1994.
(31) Allinger, N. L. *J. Am. Chem. Soc.* **1977**, *99*, 8127.

Table 1. Summary of the ^1H NMR Chemical Shifts of $[L(NH_3)_5Ru^{III}]$ at 19 °C in D_2O

L	coordn site	ionizn site	rotamer	proton	δ (ppm)	δ_{dia}[a] (ppm)	δ_{iso} (ppm)	T_1[b] (ms)	L	coordn site	ionizn site	rotamer	proton	δ (ppm)	δ_{dia}[a] (ppm)	δ_{iso} (ppm)	T_1[b] (ms)
Ade	6		*Z*	H2	20.9	7.91	13.0	1.2	Tub	6		*Z*	H2	23.1	8.13	15.0	0.9
				H8	−17.8	7.93	−25.8	0.68					H7	*e*	6.73		
Ade	6		*E*	H2	20.9	7.91	13.0						H8	−31.0	7.47	−38.4	0.5
				H8	−29.0	7.93	−36.9						H1′	6.7	6.11	0.6	12.3
Ade^-	6	1	*E*	H2	34.1	7.88	26.2						H2′	6.2	4.52	1.7	
				H8	−36.5	8.01	−44.5						H3′	5.1	4.28	0.8	
Ade^{2-}	6	1,9	*E*	H2	34.8								H4′	5.1	4.14	0.9	
				H8	−46.3								H5′	4.5	3.76	0.7	
Ado	6		*Z*	H2	21.4	8.36	13.0	4.1	Tub^-	6	1	*E*	H2	25.8	7.87	18.0	0.74
				H8	−15.7	8.46	−24.1	2.1					H7	36.7	5.83	30.9	0.74
				H1′	6.8	6.05	0.8	141					H8	−46.3	7.16	−53.5	0.41
				H2′	6.3	4.67	1.6	93					H1′	6.0	6.37	−0.3	4.6
				H3′	5.3	4.35	0.9	89					H2′	6.0	4.46	1.6	
				H4′	5.0	4.17	0.8	190					H3′	*d*	4.07		
				H5′	4.6	3.79	0.8	193					H4′	4.6	4.00	0.6	
Ado^-	6	1	*E*	H2	32.0	8.04	24.0	0.4					H5′	4.3	3.68	0.6	
				H8	−35.2	8.19	−43.4	0.29	1MeCyt	4		*Z*	H5	*d* or *e*	6.04		0.71
				H1′	5.5	5.77	−0.3						H6	40.2	7.71	32.5	2.12
				H2′	6.2	4.80	1.4	16					$CH_3(1)$	−14.1	3.37	−17.4	4.24
				H3′	4.9	4.61	0.3	171	$1MeCyt^-$	4	3	*E*	H5	−8.3	5.87	−14.2	2.02
				H4′	4.8	4.14	0.6	40					H6	63.1	7.48	55.6	0.25
				H5′	4.4	3.80	0.6	49					$CH_3(1)$	−12.6	3.3	−15.9	1.35
1MeAdo	6	1	*Z*	H2	31.7	8.40	23.3	1.59	$1,5Me_2Cyt$	4		*Z*	$CH_3(5)$	13.7	1.76	12.0	3.8
				H8	−36.6	8.41	−45.0	0.64					H6	39.7	7.24	32.4	0.95
				$CH_3(1)$	8.5	3.79	4.7						$CH_3(1)$	−23.7	3.19	−26.9	1.91
				H1′	13.5	5.99	7.5						$CH_3(1)$	−23.7	3.19	−26.9	1.91
				H2′	unresolv	4.64			$1,5Me_2Cyt^-$	4	3	*E*	$CH_3(5)$	21.1	1.86	19.2	0.17
				H3′	unresolv	4.30							H6	62.4	7.34	55.1	0.38
				H4′	unresolv	4.12							$CH_3(1)$	−9.2	3.32	−12.5	0.19
				H5′	unresolv	3.50			6-MeICyt	2			H5	*e*	5.74		
dAdo	6		*Z*	H2	21.4	8.38	13.0						$CH_3(6)$	−12.3	2.14	−14.4	0.93
				H8	−16.0	8.46	−24.5		6-MeICyt^-	2			H5	−20.2	5.66	−25.9	0.84
				H1′	7.1	6.47	0.7	31					$CH_3(6)$	−11.8	2.06	−13.9	3.7
				H2′	4.4	4.59	−0.1	98.9	Cyd	4		*Z*	H5	*e*	5.95		
				H2″	5.5	4.12	1.4	105.0					H6	25.9	7.76	18.1	20.9
				H3′	*c*	4.10							H1′	−15.4	5.81	−21.2	11.4
				H4′	4.5	3.74	0.8	67.4					H2′	6.2	4.22	2.0	73
				H5′	3.7	2.22	1.4	99					H3′	5.1	4.12	0.9	243
$dAdo^-$	6	1	*E*	H2	34.0	7.93	26.1						H4′	4.7	4.05	0.6	46
				H8	−36.0	8.11	−44.1						H5′	4.1	3.79	0.3	73
				H1′	5.8	6.23	−0.4		Cyd^-	4	3	*E*	H5	−3.1	5.95	−9.1	3.2
				H2′	4.1	4.41	−0.4						H6	31.3	7.75	23.5	1.2
				H2′	4.9	3.92	1.0						H2′	7.3	4.19	3.2	24
				H3′	4.5	3.92	0.6						H3′	5.3	4.07	1.2	254
				H4′	4.2	3.74	0.5						H4′	4.7	4.00	0.7	75
				H5′	3.4	2.54	0.8						H5′	3.1	3.78	−0.6	22
5′AMP	6		*E*	H2	21.5	8.08	13.4	4.2	5′CMP	4		*Z*	H5	*d* or *e*	6.08		
				H8	−15.8	8.38	−24.1	2					H6	27.9	8.06	19.8	
				H1′	6.7	6.02	0.7						H1′	−15.4	5.94	−21.4	
				H2′	6.3	4.66	1.6						H2′	6.5	4.80	1.7	
				H3′	5.3	4.43	0.9						H3′	5.2	4.60	0.6	
				H4′	5.1	4.32	0.7						H4′	5.0	4.20	0.8	
				H5′	4.5	4.06	0.4						H5′	4.0	4.00	0.0	
5′AMP	6	1	*Z*	H2	32.1	8.10	24.0		$5′CMP^-$	4	3	*E*	H5	−3.3	6.06	−9.3	0.94
				H8	−37.1	8.52	−45.6						H6	31.1	8.04	23.1	0.65
				H1′	5.1	6.37	−1.3						H1′	−12.9	5.92	−18.8	1.06
				H2′	5.6	4.66	1.0						H2′	7.9	4.29	3.6	
				H3′	5.2	4.43	0.8						H3′	5.5	4.29	1.2	
				H4′	4.2	4.32	−0.1						H4′	5.1	4.18	0.9	
				H5′	3.9	4.06	−0.2						H5′	2.9	4.18	−1.3	

[a] Free-ligand values. [b] Generally, values below ~4. ms were measured by the inversion-recovery technique. [c] Obscured by HOD peak. [d] Obscured by overlapping resonance. [e] Not observed and thought to be severely broadened.

While the resonances of the heterocyclic ring protons are severely shifted and broadened by the paramagnetic Ru^{III}, the more distant sugar protons, with the exception of H1′, are much less affected. The assignment of H1′ was made on the basis of its being the most affected by the paramagnetic effects of the metal ion. In the pH region of the pK_a of the complexes (Figures S3−S5), all peaks are further broadened by proton-exchange effects as well as by the rotameric equilibrium (see below). While paramagnetic line-broadening effects prevented the observation of proton−proton coupling in the 1D spectra, couplings involving H2′ through H5′ in the 2D COSY ^1H NMR made it possible to assign these resonances for the adenine nucleoside complexes.

Adenine Complexes. For the adenine nucleoside complexes, the assignments of the H2 and H8 ring protons versus the sugar protons were made by comparison with the spectrum for the analogous adenine complex. The assignment of H2 versus H8 was accomplished by the selective deuteration at the 8-position in the complex $[(8\text{-D-Ado}\kappa^{N6})(NH_3)_5Ru^{III}]$. The resonance for H2 appears substantially downfield, while that for H8 is significantly upfield, so that they bracket those of the sugar protons. The magnitudes of both δ(H2) and δ(H8) increase

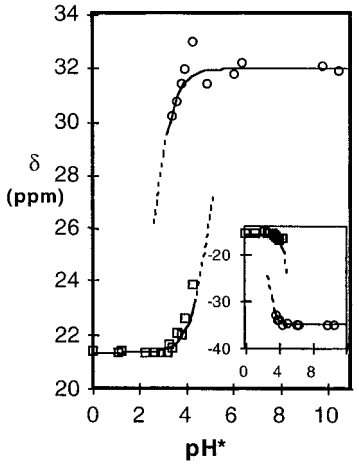

Figure 4. Plots of δ(H2) and (inset) δ(H8) versus pH* for the *Z* (squares) and *E* (circles) rotameric forms of [(Adoκ^{N6})$(NH_3)_5Ru^{III}$]. The line represents a least-squares fit using the limiting δ values, pK_a(*E*) = 2.5, and pK_a(*Z*) = 4.9.

significantly as the ligand is ionized at N1 during the course of a pH titration (see Figure 4 and Table 1).

The H2 proton resonance for the adenine complexes is shifted downfield substantially more than that for in the purine-κ^{N7} complexes, in which the metal ion is more distant.[32] On the other hand, while H8 is considerably more distant from the metal ion in the adenine-κ^{N6} than in the purine-κ^{N7} complexes, δ(H8) is shifted upfield to approximately the same degree as in the Hypκ^{N7} and Guaκ^{N7} complexes but substantially more than in the 7MeHypκ^{N9} and 7MeGuaκ^{N9} complexes.[32] As shown in Figures 4 and S3, two peaks appear for both H2 and H8 in the pH range of the spectrophotometrically (UV−vis) determined pK_a(UV−vis) for the Adoκ^{N6} complex (pH 3.4−4.3), and the relative heights of these two peaks are a reversible function of pH.

Rotamers had been predicted for the exocyclically-coordinated complexes[7,33] and are evident in the electrochemistry of these complexes.[3] Consequently, the occurrence of two peaks (Figures 4 and S3) is attributed to the presence of two rotamers, which are designated *E* (entgegen) and *Z* (zusammen) with respect to the arrangement of the Ru and imidazole ring around the C−N_{exo} bond. The separation between corresponding resonances in the two rotamers is about 20 ppm for H8 and about 10 ppm for H2. With the exception of the adenine complex (see Figure 5), the signals of both rotamers are simultaneously observed only over a relatively limited pH range, which centers on the pK_a(UV−vis),[7] so that the resonance of one rotamer predominates at low pH and that of the other predominates at high pH.

As the pH is varied, the resonance for H1′, which is the sugar proton closest to the metal center and interacts with spin density delocalized over the purine ring, varies more than those of the other sugar protons and changes position relative to H2′ (cf. values in Table 1).

In the case of the adenine complex (Figure 5), the *E*-rotamer is evident in the H8 signal over the entire pH range, while the *Z*-rotamer disappears at pH >4. For H2, the *E*-rotamer signal is also present throughout the pH range, while that for the *Z*-rotamer disappears above pH 5.5.

The H2 and H1′ resonances of the 7-deazaadenosine (tubercidin) complex are shifted downfield and are shifted to the same

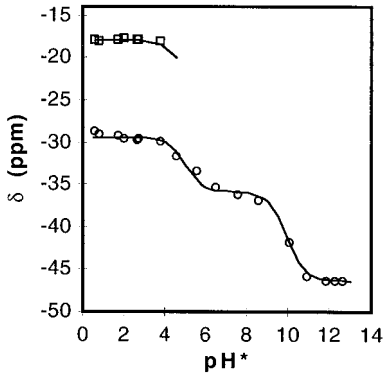

Figure 5. Plots of δ(H8) versus pH* for the *Z* (squares) and *E* (circles) rotameric forms of [(Adeκ^{N6})$(NH_3)_5Ru^{III}$] with fits to the *E* rotameric pK_a values of 4.84 ± 0.09 and 9.74 ± 0.07.

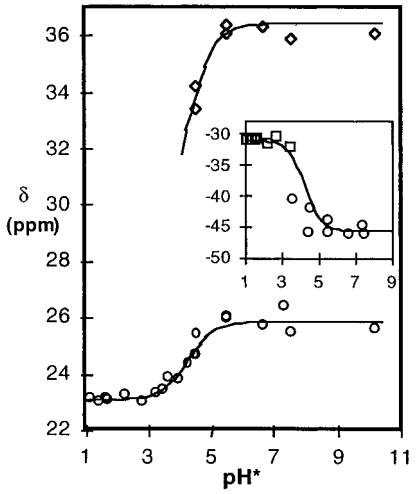

Figure 6. Plots of δ(H2) (circles) and δ(H7) (diamonds) versus pH* for [(Tubκ^{N6})$(NH_3)_5Ru^{III}$] with least-squares line fits to the pK_a value of 4.10 ± 0.07. Note that for this complex overlapping points for the same proton are not evident. Nevertheless, the resonance for H7 is too severely broadened at low pH to be observed under the conditions used. The inset is a plot of δ(H8) versus pH.

extent as the respective resonances in the adenosine complexes (cf. Table 1). On the other hand, δ(H8) is shifted 15 ppm more upfield than those of the adenosine complexes. The tubercidin complex also appears to exhibit a separation in the H8 resonance around pH 3.5 (Figure 6, inset); however, two peaks are not evident for any proton in the same NMR sample (see Figure 6). The resonance for H7 is severely broadened and shifted downfield but is distinct at high pH; however, it becomes so broadened as to be unobservable at pH <4.5 (see Figure 6). Upon deprotonation at N1, the H2, H8, and H1′ peaks are shifted less downfield and upfield, respectively, than those in the adenosine complexes.

Figure S7 (Supporting Information) shows the correlation between A_H values and the δ_{iso} values for the two ring protons in $[L(NH_3)_5Ru^{III}]$, where L = *Z*-Cydκ^{N4}, *Z*-Adoκ^{N6}, *E*-Cyd$^-\kappa^{N4}$, and *E*-Ado$^-\kappa^{N6}$.

Cytosine Complexes. Assignments of the H5 and H6 resonances in these ligands were determined by observing that the upfield resonance in the spectrum of [(1MeCyt)$(NH_3)_5Ru^{III}$] was absent from the spectrum of [(1,5Me_2Cyt)$(NH_3)_5Ru^{III}$]. Sugar H1′ peaks were assigned on the basis of their upfield shifts and line widths, which are comparable to those for the N1 methyl group in the complex of 1MeCytκ^{N4}.

Similar to the adenine complexes, the cytosine species also exhibit *E*- and *Z*-rotamers (see Table 1 and Figures 7 and S5), which appear in the ^{1}H NMR spectra as two sets of peaks at

(32) Bailey, V. M.; LaChance-Galang, K. J.; Doan, P. E.; Clarke, M. J. *Inorg. Chem.*, in press.
(33) Clarke, M. J.; Dowling, M. G.; Brennan, T. F.; Garafalo, A. F. *J. Am. Chem. Soc.* **1979**, *101*, 223−225.

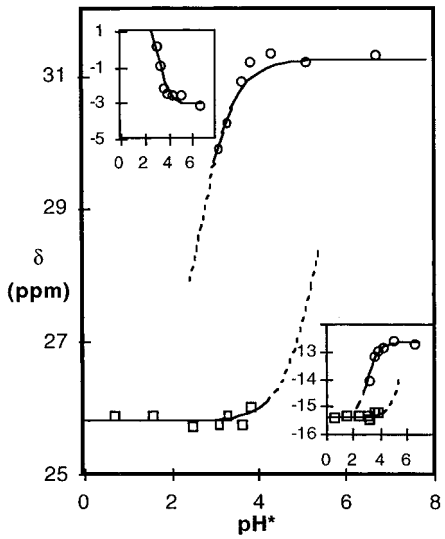

Figure 7. Plots of δ(H6), δ(H5) (upper inset), and δ(H1′) (lower inset) versus pH* for the *Z* (squares) and *E* (circles) rotameric forms of [(Cyd^{N4})$(NH_3)_5Ru^{III}$]. The lines for δ(H6) and δ(H1′) represent least-squares fits using the limiting δ values and pK_a(*E*) = 2.6 and pK_a(*Z*) = 5.3. The line fits for δ(H5) and δ(H1′) use pK_a = 3.0.

pH ∼ pK_a(UV−vis) for H6 and the alkyl protons on the first carbon connected to N1. By analogy to the adenine complexes, *Z* designates the metal ion's being on the C5 side of the ligand, while the *E* form occurs at higher pH, when the metal ion hydrogen-bonds to N3.[8]

The neutral ligand (low pH) forms of the Cydκ^{N4} and 1MeCytκ^{N4} complexes exhibit severely broadened H5 resonances that undergo an upfield shift upon ionization from N3 (see Figure 7). The H6 signals for the Cydκ^{N4} and 1MeCytκ^{N4} neutral ligand complexes are quite broadened and shifted downfield by 18−32 ppm relative to that of the free ligand and undergo further downfield shifts of ∼5 and 23 ppm, respectively, upon N3 ionization (cf. Table 1), which also shifts both δ(H1′) and $\delta(CH_3(1))$ slightly downfield by about 1.5 ppm.

For [$(1,5Me_2Cyt)(NH_3)_5Ru^{III}$], the resonances for $CH_3(1)$, $CH_3(5)$, and H6 are distinct at pH values significantly above or below the pK_a. Upon ionization at N3, all the protons undergo significant downfield shifts relative to the neutral ligand complex. In the pH range of the pK_a, the H6 and the $CH_3(1)$ peaks become so severely broadened that the shifts cannot be ascertained.

Sugar Protons. While the sugar proton assignments for the adenosine and deoxyadenosine complexes were possible through 2D COSY ^{1}H NMR (Figures S1 and S2), the very short T_1 values of the Cydκ^{N4} and 5′CMPκ^{N4} complexes prevented the appearance of cross peaks in their 2D COSY spectra. Consequently, sugar assignments were made by analogy to those of the adenosine complex. Unlike those for the κ^{N7} complexes of guanosine and inosine,[32] δ(H1′) for the adenosine complexes exhibits a very small shift (0.25−0.75 ppm) relative to the free ligand at neutral pH and both δ and δ_{iso} (1.4−1.65 ppm) for H2′ are greater than those for H1′ (cf. Table 1). The resonances for H3′ through H5′ in the Adeκ^{N6} complex are shifted by 0.30−0.95 ppm, relative to the free ligand, while those for the 5′AMPκ^{N6} complex are shifted 0.15−0.95 ppm.

In contrast to the case of the 5′GMPκ^{N7} and 5′IMPκ^{N7} complexes,[32] there is no increase in δ(H5′) for the 5′AMPκ^{N6} complex compared to that of the Adoκ^{N6} complex. As the pH is increased, the resonances of all the sugar protons (except H2′) shift upfield with δ(H1′) changing more than those of the other sugar protons and crossing over the H2′ peak. The phenomenon

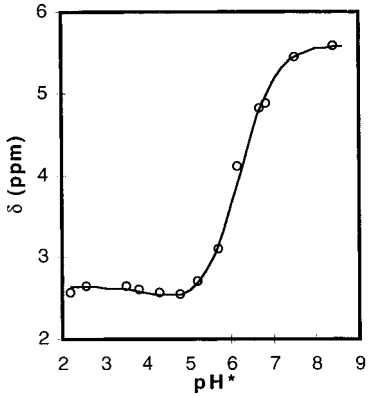

Figure 8. Plot of ^{31}P NMR δ(P) versus pH* for [(5′AMPκ^{N6})$(NH_3)_5Ru^{III}$] fit with pK_a values of 4.1 (N1) and 6.03 (phosphate).

of H1′ exhibiting a negative δ_{iso} upon N1 ionization while δ_{iso} for all other sugar protons remains positive is common to all complexes with adenine ligands (Ado, dAdo, 5′AMP).

In the Cyd and 5′CMP complexes, two rotameric forms are evident in doubled peaks for the ribose protons, except H4′, when pH ∼ pK_a(UV−vis). Unlike those of the adenine complexes, the H1′ resonances of the neutral ligand cytidine complexes are shifted substantially upfield (δ ∼ −15 ppm). The δ_{iso} values are downfield somewhat more for H2′ (1.6−4.0 ppm) than for H3′−H5′ (usually 0.05−1.3 ppm; Table 1). Upon N3 ionization, which favors the *E*-rotamer, of the cytidine complexes, H1′−H3′ resonances all undergo downfield movements, with the largest (∼3 ppm) being for H1′, while the H5 signal is shifted upfield. Only a single peak was evident for H4′ over the entire pH range, and this shifted very slightly downfield upon N3 ionization. No particular trend in T_1 values for the exocyclically-coordinated complexes emerged as a function of pH.

pK_a Values. Since the limiting shift values for an individual rotamer are known only for the complex with *E*-Adeκ^{N6}, its pK_a values can be reliably determined as 4.84 ± 0.09 and 9.74 ± 0.07 from the NMR data shown in Figure 5 for ionization from the N1 and N7/N9 sites, respectively.[7] These compare well with the previously determined pK_a(UV−vis) values of 4.54 and 9.88,[7] which do not discriminate between rotamers; however, the NMR data in Figure 5 suggest the pK_a(UV−vis) values should be weighted toward the *E*-rotamer.

Fitting the data shown in Figure 4 for δ(H2) and δ(H8) of the Adoκ^{N6} complex (and assuming the same end-point shift values for both rotamers), we estimate pK_a(*E*) and pK_a(*Z*) as 2.5 and 4.9, respectively, for ionization at N1.[7] For the 5′AMPκ^{N6} complex (Figure S6), the N1 pK_a(*E*) and pK_a(*Z*) values are 2.8 and 4.4, respectively. Similar estimates using the data shown in Figure 6 for δ(H1′) and δ(H6) of the Cydκ^{N4} complex yield N3 ionization pK_a(*E*) and pK_a(*Z*) values of 2.6 and 5.3, respectively, while these values for the 5′CMPκ^{N4} rotamers are 3.2 and 4.9, respectively. If a smaller difference in δ values between the different ionization states is assumed, the difference between the estimated pK_a(*E*) and pK_a(*Z*) values (ΔpK_{aEZ}) decreases. The pK_a (4.10 ± 0.06) derived from the data in Figure 6 for the Tubκ^{N6} complex is in excellent agreement with the pK_a(UV−vis) of 4.00.[7]

^{31}P NMR. In contrast to the κ^{N7} complexes of 5′GMP and 5′IMP, the 5′AMPκ^{N6} and 5′CMPκ^{N4} complexes exhibit little change in ^{31}P chemical shift relative to the free nucleotides (see Figures 8 and 9 and Table 2). The phosphate pK_a values are 6.03 ± 0.05 and 6.23 ± 0.03 for the 5′AMPκ^{N6} and 5′CMPκ^{N4} complexes, respectively, only slightly different from the value of 6.3 exhibited by the free nucleotides.[34] The lower pK_a evident

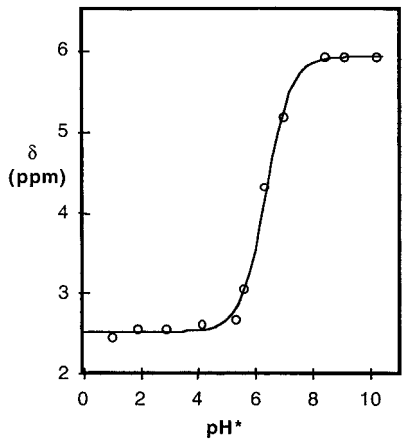

Figure 9. Plot of ^{31}P NMR δ(P) versus pH* for [(5′CMPκ^{N4})(NH$_3$)$_5$Ru^{III}] fit with pK_a = 6.23.

Table 2. ^{31}P NMR Chemical Shifts of [L(NH$_3$)$_5$Ru^{III}] at 19 °C in D$_2$O

L	δ (ppm)	δ_{dia}[a] (ppm)	δ_{iso} (ppm)
5′AMP	2.57	1.08	1.49
5′AMP^{2-}	5.59		
5′CMP	2.53		
5′CMP^{2-}	5.92	5.16	0.76

[a] δ_{dia} is taken as δ for the free ligand.

Table 3. Wyberg Bond Indices and Bond Lengths for Pentaammineruthenium(III) Complexes of κ^{N7}- and κ^{N4}-Coordinated Nucleosides[a]

complex	Ru−N (Å)	Wyberg constant
[(Guoκ^{N7})(NH$_3$)$_5$Ru]$^{3+}$	2.071	0.70
[(Inoκ^{N7})(NH$_3$)$_5$Ru]$^{3+}$	2.087	0.69
Z-[(Cydκ^{N4})(NH$_3$)$_5$Ru]$^{3+}$	1.983	0.81
E-[(Cyd$^-\kappa^{N4}$)(NH$_3$)$_5$Ru]$^{2+}$	1.983	0.82

[a] Bond distances are derived from refs 8, 36, and 51.

in varying the pH of the 5′AMPκ^{N6} complex (Figure 8) is estimated as 4.2, which compares well with the average value for pK_a(*E*) and pK_a(*Z*) of 3.8 attributed to ionization from N1 and is accompanied by UV−vis spectral changes in the π−d$_\pi$ LMCT range consistent with such ionization.[35,36]

EPR. EPR *g* values for the neutral-ligand Adoκ^{N6} and Cydκ^{N4} complexes, respectively, are $g_\perp$ = 2.534 and 2.514 and $g_{||}$ = 2.096 and 2.095. At pH 8, these become $g_\perp$ = 2.477 and 2.524 and $g_{||}$ = 1.668 and 1.557, respectively.

Paramagnetic Effects and MO Calculations. While the magnetic axes could not be unequivocally assigned, the Ru−N$_{exo}$ axis was chosen as the unique (*z* or ⊥) axis and eq 1 was used to determine dipolar shifts, which were then used to estimate the contact shifts. Regardless of how the magnetic axes were assigned, the values listed in Table S1 indicate that contact shifts dominate for the protons on the heterocyclic rings and on the first alkyl carbon. A good correlation is evident in Figure S7 between the calculated A_H(INDO/1) values and the δ_{iso} values for the two ring protons in [L(NH$_3$)$_5$Ru^{III}], where L = *Z*-Cydκ^{N4}, *Z*-Adoκ^{N6}, *E*-Cyd$^-\kappa^{N4}$, and *E*-Ado$^-\kappa^{N6}$. Table 3 demonstrates that the exocyclically-bound complexes, which have significantly shorter Ru−N$_L$ bond distances, have larger Wyberg bond indices as derived from INDO/1 calculations[28,37,38] than the endocyclically coordinated species.

Discussion

The $^2T_{2g}$ ground states of low-spin d^5 ions such as Ru^{III} and Fe^{III} often generate short electronic relaxation times (T_{1e} < 10^{-8} s) and relatively long nuclear relaxation times ($T_1 \simeq 10^{-2}$−10^{-4} s), which can give well-resolved ^{1}H NMR spectra[39] but often obscure proton−proton coupling. INDO calculations for *trans*-(Im)$_2$Fe^{III}-porphyrin[40,41] and *trans*-[L(Im)(NH$_3$)$_5$Ru^{III}] systems[42] indicate that ligand-to-metal π-charge transfer accounts for spin transfer into the highest bonding orbital of the axial imidazoles. This is consistent with the UV−vis LMCT bands of [L(NH$_3$)$_5$Ru^{III}], where L = pyridine,[43] imidazole,[44] endocyclically-coordinated purine,[36] and exocyclically-coordinated adenine and cytosine,[7] that are indicative of π−d$_\pi$ interactions. Polypyridyl complexes of Ru^{III} relative to those of Fe^{III} show significantly greater π-spin density delocalization, which arises from the larger extension of 4d relative to 3d orbitals.[45,46]

Cytosine Complexes. In keeping with this, the estimated dipolar shifts and contact shifts listed in Table S1 for the complexes with Cydκ^{N4} and Cyd$^-\kappa^{N4}$ indicate that the large δ_{iso}(H5) and δ_{iso}(H6) values for these and related complexes can be attributed to large contact shift contributions. High delocalization of spin density throughout the cytidine ring is consistent with the appreciable π-bonding evident in the relatively high Wyberg bond index for these complexes and the short Ru−N4 bond distance in the crystal structure of [(1MeCyt$^-\kappa^{N6}$)(NH$_3$)$_5$Ru^{III}].[8,47] In this structure, partial π-bonding between Ru and N4 occurs at the expense of the partial π-bond between N4 and C4. Partial π-bonding is also evident in the INDO/1 calculations of these complexes and accounts for the good correlation between the δ_{iso} values for the ring protons and their calculated A_H values as shown in Figure S7.

The spin density pattern for the cytosine complexes (Figure S6) is similar to those observed for analogous pyridine complexes[32] in that the resonance for the *ortho* proton (δ(H5)) is upfield, while that for the *meta* proton (δ(H6)) is downfield (see Table 1); but the magnitudes of these shifts are much larger than those for the corresponding protons in the pyridine complexes.[32] The relative ordering of $|\delta_i s_o|$ for these protons is H6 > H1′(CH$_3$) ≫ H5, which differs from those for the pyridine complexes, where H2,6 > H4 ≫ H3,5, and the 6MeICyt complex,[48] where H5 ≫ CH$_3$(6). The enhanced chemical shift of H6 in the cytosine complexes relative to those for the analogous protons (H3,5) in the pyridine complexes may arise from contributing resonance structures in the former as shown in Figure 10. Such resonance depletes electron density

(34) Dawson, R. M. C.; Elliott, D. C.; Elliott, W. H.; Jones, K. M. *Data for Biochemical Research*, 2nd ed.; Oxford University Press: Oxford, U.K., 1969; p 158.
(35) Clarke, M. J.; Taube, H. *J. Am. Chem. Soc.* **1974**, *96*, 5413−5419.
(36) Kastner, M. E.; Coffey, K. F.; Clarke, M. J.; Edmonds, S. E.; Eriks, K. *J. Am. Chem. Soc.* **1981**, *103*, 5747−5752.
(37) Anderson, W. P.; Cundarai, T. R.; Drago, R. S.; Zerner, M. C. *Inorg. Chem.* **1990**, *29*, 1−3.
(38) CAChe Scientific. *ZINDO 2.8*; Terra Pacific Writing Corp.: Beaverton, OR, 1991.
(39) Jesson, J. P. In *NMR of Paramagnetic Molecules*; La Mar, G. N., Horrocks, W. D., Holm, R. H., Eds.; Academic Press: New York, London, 1973; pp 2−51.
(40) Satterlee, J. D.; La Mar, G. N. *J. Am. Chem. Soc.* **1976**, *98*, 2804−2808.
(41) Chacko, V. P.; La Mar, G. N. *J. Am. Chem. Soc.* **1982**, *104*, 7001−7007.
(42) LaChance-Galang, K. J.; Doan, P. E.; Clarke, M. J.; Rao, U.; Yamano, A.; Hoffman, B. *J. Am. Chem. Soc.* **1995**, *117*, 3529−3538.
(43) Curtis; Meyer, T. J. *Inorg. Chem.* **1982**, *21*, 1563.
(44) Sundberg, R. J.; Bryan, R. F.; Taylor, I. F.; Taube, H. *J. Am. Chem. Soc.* **1974**, *96*, 381−392.
(45) Desimone, R. E.; Drago, R. S. *J. Am. Chem. Soc.* **1970**, *92*, 2343−2352.
(46) Kurland, R. J.; McGarvey, B. R. *J. Magn. Reson.* **1970**, *2*, 286−301.
(47) Clarke, M. J. *Inorg. Chem.* **1980**, *19*, 1103−1104.
(48) LaChance-Galang, K. J. Ph.D. Thesis, Boston College, 1995.

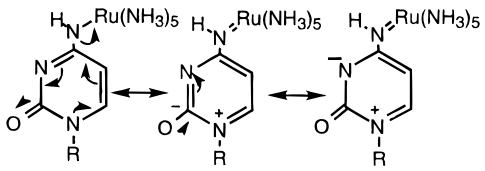

Figure 10. Resonance structures in $[(Cyt\kappa^{N4})(NH_3)_5Ru^{III}]$.

on N1, thereby placing positive spin density on it; this polarizes negative spin density on C6, which, in turn, polarizes positive spin density on H6.

In contrast to the case of Adoκ^{N6} complexes, δ(H1′) is significantly more upfield due to a greater transfer of spin density owing to the resonance effect (Figure 10), the *para* position of N1 relative to the Ru^{III} position on the ring, and the shorter N_{exo} to glycosidic N distance in cytidine relative to adenosine. For the methyl-substituted Cytκ^{N4} derivatives, δ-(CH_3(1)) is shifted upfield, while δ(CH_3(5)) is shifted downfield, again reflecting an alternating spin density around the ring. Increasing the size of the substituent on N1 and increasing the number of ring substituents also tend to enhance the upfield shift of the alkyl protons on the first carbon attached to N1.

Z- and *E*-rotamer formation (Figure 2) is apparent in the ^{1}H NMR spectra of the cytosine complexes by the appearance of distinct peaks for H6 and the alkyl protons at high and low pH but two highly broadened peaks for each of these at pH ∼ pK_a(UV−vis). The extreme broadening of the H5 peak at low pH for all the complexes arises from the proximity of the paramagnetic Ru^{III} to H5 in the *Z*-rotamer. Unlike the case of the adenine complexes (see below), for which the *Z*-rotamer can be stabilized by hydrogen-bonding to N7, Ru is more likely to swing between rotameric positions at low pH in the cytosine complexes. The oscillating magnetic field so produced may account for δ(H5) often being unobservable at low pH (Table 1).

While three distinct peaks for CH_3(1), CH_3(5), and H6 are observed at either end of the pH range for the 1,5Me_2Cytκ^{N4} complex, the severe broadening of these resonances at pH ∼ pK_a is consistent with rapid rotation due to the instability of the *Z*-rotamer, which is sterically inaccessible because of the CH_3(5).

Similarly, space-filling models for the 6MeICyt^{N4} complex show that, at low pH, when both N1 and N3 are protonated, neither rotamer is stabilized relative to the other. Hence the Ru^{III} probably spends more time swaying between positions outside the plane of the ring, so that the severe broadening of the *para* H5 resonance at pH < pK_a likely results from rapid variations in its magnetic field as differing amounts of spin density are transferred through modulations in the Ru−N4 π-bond. At pH values between the pK_a's of the two nitrogens, the H5 resonance emerges with the formation of hydrogen bonds between the coordinated ammine and the ionized N1. At pH > pK_a of both nitrogens, δ(H5) broadens again because there is a greater transfer of spin density and possibly also because the Ru^{III} can hydrogen-bond to either N1 or N3, so that the two rotamers are of approximately equal energy, which minimizes the E_a between them.[48]

Adenine Complexes. Regardless of the assignment of the magnetic axes in $[(Ado\kappa^{N6})(NH_3)_5Ru^{III}]$, the largest magnitude of a dipolar shift, $|\delta_{dip}|$, calculated for a ring proton is 0.3. Consequently, the large δ_{iso}(H8) and δ_{iso}(H2) values for this and related complexes can be attributed to contact shift contributions. As in the cytosine complexes, high delocalization of spin density throughout the adenine ring is consistent with π-bonding between Ru^{III} and N6.[8,47]

Despite exocyclic coordination, which introduces the spin at a different site and increases the through-bond distance to the imidazole ring, the calculated spin density pattern (see Figure S6) in the imidazole portion of the ring is analogous to that in the purine-κ^{N7} complexes. Moreover, the H8 resonance in these complexes shows direction, magnitude, and line broadening similar to those of H8 in the Inoκ^{N7} and Hypκ^{N7} complexes. This is probably due to the greater π-bonding in the exocyclic complexes, so that a comparable amount of spin density is transferred into the imidazole ring as the π-electron-rich imidazole donates electron density to the electron-deficient pyrimidine ring. This interpretation is in accord with the calculated A_H(H8) being greater than A_H(H2) for the *E*-rotamer (cf. Table S1).

As with the purine-κ^{N7} complexes, δ_{iso}(H8) is progressively less shifted with increasing size of the N9 substituent (H > deoxyribose > ribose > ribose monophosphate) for the neutral ligand *Z* complexes; however, these shifts are small by comparison. This order also holds for $|\delta_{iso}$(H2)|.

Both the direction and magnitude of δ(H2) differ between κ^{N6} adenine and κ^{N7} hypoxanthine complexes, which must arise from the introduction of the spin density at a different site in the aromatic ring. Both δ(H2) and δ(H8) shift substantially further downfield and upfield, respectively, upon methylation at N1 of adenosine, which probably arises from a slight increase in π-bonding to the metal due to the electron-donating ability of the methyl group.

Rotamer formation, which is evident in two current peaks in the electrochemistry of these complexes,[3,7,49,50] is also reflected in their ^{1}H NMR spectra. The individual peaks for H2 and H8 at low pH, where N1 is protonated, are due to the formation of the *Z*-rotamer (see Figure 3) as Ru^{III} is sterically induced to swing over to the imidazole portion of the purine, where a coordinated ammine can hydrogen-bond to N7. At higher pH, another set of H2 and H8 peaks occurs more downfield for H2 and more upfield for H8. These arise due to the formation of the *E*-rotamer as N1 ionizes and stronger hydrogen-bonding between the coordinated ammine and the anionic N1 comes into play to bring Ru^{III} to the N_{endo} side of the purine. At pH ∼ pK_a(UV−vis), approximately equal concentrations of both rotamers occur with enhanced line widths due to proton exchange broadening.

The dependence of the rotameric equilibria on hydrogen-bond formation involving either N1 or N7 is seen in the spectra of the 1MeAdoκ^{N6} and the Tubκ^{N6} complexes. Methyl substitution at N1 sterically prevents formation of the *E*-rotamer, so that the 1MeAdoκ^{N6} complex exhibits a single set of peaks throughout the pH range. Since hydrogen-bonding to the imidazole ring cannot occur with tubericidin so as to stabilize the *Z*-rotamer, at low pH the metal ion probably oscillates between the two protonated positions, generating a varying magnetic field, which rapidly relaxes nearby nuclei, leading to extreme broadening of the H7 peak at low pH. Consequently, the tubercidin does not exhibit two sets of peaks at pH ∼ pK_a(UV−vis) and the pK_a(NMR) derived from the data in Figure 6 agrees well with the pK_a(UV−vis).[7]

The adenine complex uniquely exhibits the presence of the *E*-rotamer throughout the pH range (see Figure 5). This

(49) Galang, R.; Clarke, M. J. Unpublished results, 1990.
(50) Clarke, M. J.; Galang, R. G.; Rodriguez, V. M.; Kumar, R.; Pell, S.; Bryan, D. M. In *Proceedings of the 5th International Symposium on Platinum Compounds in Cancer Chemotherapy*; Nicolini, M., Ed.; Kluwer Publishing: Boston, MA, 1987; pp 582−600.
(51) Clarke, M.; Bailey, V. M.; Doan, P.; Hiller, C.; LaChance-Galang, K. J.; Daghlian, H.; Mandal, S.; Bastos, C.; Lang, D. *Inorg. Chem.* **1996**, *35*, 4896−4903.

probably arises from the tautomeric equilibria of the imidazole proton between N7 and N9 (Figure S8). While the N9 tautomer enables hydrogen-bonding to N7 to stabilize the *Z*-rotamer, the N7-tautomeric form pushes Ru^{III} back to the less sterically hindered pyrimidine side. Because of the closer proximity of the metal ion to N1, this site may ionize, thereby stabilizing the *E*-rotamer, or, at lower pH, result in an oscillating structure as with tubercidin.

Rotameric pK_a Equilibria. Since the increase in the acidity (ΔpK_a) of L in $[L(NH_3)_5Ru^{III}]$, where L = imidazole, purine, and pyrimidine derivatives, varies according to the empirical relation[36]

$$\Delta pK_a = \frac{135}{R^2} - 2.7 \qquad (2)$$

where R (Å) is the distance between Ru^{III} and the ionization site, the difference in pK_a values of the N_{endo} site (ΔpK_{aEZ}) should differ substantially between the two rotameric forms. The average ΔpK_{aEZ} value for the complexes of Cytκ^{N4}, 5′CMPκ^{N4}, Adoκ^{N6}, and 5′AMPκ^{N6} is 2.3, which is realistic compared with the value of 5.6 estimated from eq 2.[52] Similarly the average values of 4.0 and 3.9 for pK_a(Cydκ^{N4}(N3)) and pK_a(Adoκ^{N6}(N1)), respectively, are in the range of those measured at 23 °C by UV−vis spectroscopy (which essentially does not discriminate between the rotamers) of 3.2 and 3.6, respectively.[7] The overestimation of ΔpK_{aEZ} by eq 2 may have to do with Boltzmann populations involving structures in which Ru is out of the plane of the heterocyclic ring, which affect not only R but also the degree of π-interaction.

Glycosyl Protons. The patterns of sugar resonances for the Adoκ^{N6} and 5′AMPκ^{N6} complexes are similar for the *Z*-rotamer (H1′ > H2′ > H3′ > H4′ > H5′) and for the *E*-rotamer (H2′ > H1′ > H3′ > H4′ > H5′), except that δ(H1′) switches position relative to δ(H2′). On the other hand, the pattern of the sugar resonances of the deoxyadenosine complex (H1′ > H2″ > H3′ > H4′ > H2′ > H5′) is invariant with pH. This difference may arise as ribose rings often prefer the *C3′-endo* conformation, because the electronegative C2′−OH favors the axial position;[17] whereas, the deoxyadenosine complex may have a higher population of the *C2′-endo* conformation.

A notable difference in the ^{1}H NMR spectra of the adenosine complexes as compared to the cytidine and κ^{N7} guanosine and inosine nucleoside complexes[32] is the absence of the characteristically large $|\delta_{iso}$(H1′)|. This difference in magnitude for δ_{iso}(H1′) may result from the longer Ru−H1′ through-bond distance in Adoκ^{N6} but probably has more to do with the distribution of spin density within the imidazole ring, as the δ_{iso}(H8) values are similar to those of the κ^{N7} purine complexes. Consistent with this, the $|\delta_{iso}$(H1′)| values for the Cydκ^{N4} complexes are substantially greater than those for the Inoκ^{N7} and Guoκ^{N7} complexes, since the higher transfer of spin density into the nucleoside through greater π-bonding more than offsets the somewhat longer through-bond distance to H1′. The difference in sign for δ_{iso}(H1′) for the cytidine complexes relative to the Adoκ^{N6}, Inoκ^{N7}, and Guoκ^{N7} complexes also must arise from the site of H1′ on the aromatic ring.

Since the patterns for the sugar H2′−H5′ resonances of the Cydκ^{N4} and 5′CMPκ^{N4} complexes are similar to those for the Adoκ^{N6} and 5′AMPκ^{N6} complexes (H2′ > H3′ > H4′ > H5′), a similar preference for an *anti* orientation about the glycosidic bond may be suggested.

Phosphate Interactions. As indicated by the relatively unperturbed phosphate pK_a and $\delta_{iso}(^{31}P)$ values, there is little interaction between the Ru^{III} center and the nucleotide phosphates. Computer-generated structural models of the nucleotide complexes show that the through-space Ru^{III}−P distances are much larger in the 5′AMPκ^{N6} (>7.6 Å) and 5′CMPκ^{N4} (>6.3 Å) complexes than in the 5′GMPκ^{N7} and 5′IMPκ^{N7} complexes (∼2.2−3.9 Å) and are well beyond a reasonable distance for hydrogen-bonding. The small values of δ_{iso} for the sugar protons in the 5′AMPκ^{N6} complex compared with the κ^{N7} nucleotides,[32] which are likely ammine−phosphate hydrogen-bonded, similarly indicate the absence of any significant interaction between the ruthenium and phosphate centers.

Conclusion. Endocyclic (κ^{N7}) versus exocyclic (κ^{N6}) binding in purines is distinguished by the direction of δ(H2) (upfield for κ^{N7} and downfield for κ^{N6}) and the relative magnitude of δ(H1′) ($\kappa^{N7} \gg \kappa^{N6}$). Upon ionization of the purine, δ(H1′) moves further downfield for κ^{N7} complexes, while for κ^{N6} complexes it tends to move slightly back upfield. The presence of two sets of peaks for the H1′ and H2 and (in κ^{N6} adenine complexes) H8 resonances at pH ∼ pK_a(UV−vis) indicates two rotamers with distinct acid−base behavior, whose difference in acidities is somewhat overestimated by eq 2, perhaps because of Boltzmann populations involving structures in which Ru is out of the plane of the heterocyclic ring. The spin density pattern in the pyrimidine ring of the exocyclically coordinated complexes is similar to that of $[py(NH_3)_5Ru]^{3+}$.[32] By comparison with pyridine complexes,[32] N_{exo} versus N_{endo} pyrimidine linkage isomers might be determined by the magnitude of the resonances of the ring protons, as the greater π-bonding in the former generates larger $|\delta_{iso}|$ values.

Acknowledgments. This work was supported by PHS Grant GM26390. We are grateful to Prof. Hans Van Willigen (University of Massachusetts, Boston) who generously provided the EPR spectra.

Supporting Information Available: COSY spectra of the sugar protons in $[(Ado\kappa^{N6})(NH_3)_5Ru^{III}]$ and $[(dAdo\kappa^{N6})(NH_3)_5Ru^{III}]$ in D_2O, ^{1}H NMR spectra of $[(Ado\kappa^{N6})(NH_3)_5Ru]^{3+}$, $[(Cyd\kappa^{N6})(NH_3)_5Ru]^{3+}$, and $[(5'AMP\kappa^{N6})(NH_3)_5Ru]^{3+}$ as a function of pH, calculated spin density patterns for $[L(NH_3)_5Ru^{III}]$, a plot of δ_{iso} values for the ring protons versus calculated A_H(INDO/1) for $[L(NH_3)_5Ru^{III}]$, tautomeric structures of $[(Ade\kappa^{N6})(NH_3)_5Ru]^{3+}$, and a table of A_H values for the ring protons of $[L(NH_3)_5Ru^{III}]$ (L = derivatives of adenosine and cytidine) (9 pages). Ordering information is given on any current masthead page.

IC9610142

(52) The estimation of $\Delta pK_{aEZ} = \Delta pK_a(Z) - \Delta pK_a(E)$ by eq 2 employed R_E = 3.16 Å and R_Z = 4.15 Å, which are derived from idealized structures with bond distances taken from the structure of $[(1MeCyt^-\kappa^{N4})(NH_3)_5Ru^{III}]^{2+}$.[8,47]